

Influence of Cross-Linking on Probe Dynamics in Semidilute Polystyrene Systems

Markus Susoff and Wilhelm Oppermann*

Institute of Physical Chemistry, Clausthal University of Technology, Arnold-Sommerfeld-Strasse 4, 38678 Clausthal-Zellerfeld, Germany

Received August 17, 2010; Revised Manuscript Received October 4, 2010

ABSTRACT: Fluorescently labeled polystyrene (PS) tracer molecules are enclosed in a semidilute, entangled solution of PS matrix polymers. The latter carry photo-cross-linkable groups such that the matrix can be successively cross-linked by UV-irradiation. The diffusion coefficient of the labeled tracer chains is measured via FRAP at every stage of the cross-linking process during the transition from sol to gel. In the sol state, significant deviations from the reptation predictions appear unless the matrix chains are considerably longer than the tracer chains. Cross-linking of the matrix chains results in a more or less pronounced decrease of the tracer diffusion coefficient, occurring gradually with rising conversion of the cross-linking reaction, while the observed dependencies of the tracer diffusion coefficient on tracer molecular weight and on matrix concentration converge to what is predicted by reptation theory.

Introduction

The dynamics of linear macromolecules in highly entangled systems is largely governed by topological constraints. An adequate theoretical approach was achieved by the notion that a given chain is confined to a tubelike region defined by neighboring chains and can only relocate its position or rearrange its conformation by reptation, i.e., curvilinear diffusion along its own contour. This model was first proposed by de Gennes.^{1–4} The average time necessary for complete rearrangement of conformation, τ_{rep} , and the macroscopic diffusion coefficient, D , were shown to vary with chain length (or molar mass M) as

$$\tau_{\text{rep}} \sim M^3 \quad (1)$$

$$D \sim R^2 / \tau_{\text{rep}} \sim M^{-2} \quad (2)$$

where R is a measure of coil size.

These predictions largely agree with experimental results when melts or concentrated solutions consisting of very long polymers chains are considered and also for long linear chains entrapped in gels.⁵ On the other hand, systematically deviating results have also been reported, and it was suggested that pure reptation is only one of several mechanisms of chain dynamics. Another one could be renewal of the tube (or constraint release) arising from the motion of the surrounding chains; a third one could be path length fluctuations.^{6–10}

A clearer picture evolves when studying the tracer diffusion coefficient D_{tr} of a test chain of molecular weight M in a matrix of surrounding chains having molecular weight P (chemically identical to or different from the tracers). Experimental results imply that the pure reptation hypothesis works well only when sufficiently long tracer chains in a matrix of much longer chains or in a network are considered.^{11,12} In this situation, the constraints can be regarded fixed, in consent with de Gennes' original model, because their lifetime is longer than the reptation time of the test

chain. However, when P/M is less than 3–5, the constraint release mechanism becomes important or even dominant. Defining the relaxation time of the tube as τ_{cr} , the tracer diffusion coefficient may then be written as⁷

$$D_{\text{tr}} \sim R^2 (1/\tau_{\text{rep}} + 1/\tau_{\text{cr}}) \quad (3)$$

The molecular weight of the matrix polymer, P , strongly affects τ_{cr} .

When the reptation hypothesis is applied to semidilute entangled solutions, their concentration, c (specifically, the matrix concentration), obviously becomes a crucial quantity influencing the tracer diffusion coefficient. Furthermore, solvent quality has to be taken into account. The corresponding prediction is

$$D_{\text{tr}} \sim M^{-2} c^{-k} P^0 \quad (4)$$

with $k = 1.75$ for a good (athermal) solvent and $k = 3$ for a θ -solvent.^{3,5} Applying mean-field arguments for excluded volume interaction to the basic scaling and reptation theory prompted Schaefer et al. to define a third regime, the so-called marginal solvent, where $k = 2.5$ – 2.75 .^{13,14}

While reptation certainly is important in melts, its significance in semidilute solutions has been questioned.⁵ With increasing dilution, the molecular weight between entanglements rises and the tube diameter rises, too. That is why only extremely long chains can be expected to undergo reptation in this situation. However, a clear proof or disproof of reptation has not been achieved. In part, this may be due to the difficulties posed by the various scaling exponents predicted for the concentration dependence in different regimes.

Several investigations on the dynamics of polymers in melts as well as in semidilute and concentrated solutions and in gels agree, at least in part, with the scaling laws of reptation. Different techniques have been applied, such as forced Rayleigh scattering (FRS),^{11,12,15–21} dynamic light scattering (DLS),^{15,22–35} pulsed field gradient NMR,^{36–41} fluorescence recovery after photobleaching (FRAP),^{30,42–45} fluorescence correlation spectroscopy (FCS),^{46–48} and single molecule tracking.⁴⁹ In particular, the

*Corresponding author. E-mail: wo@tu-clausthal.de.

M^{-2} prediction could be confirmed, e.g., by studies of Wesson et al., Wheeler et al., and Nemoto et al. on the dynamics of polystyrenes enclosed in polymer solutions at different concentrations.^{12,18,21,32} Inspection of the concentration dependence of the diffusion coefficient seems to be more difficult than studying the molecular weight dependence. Only a few groups verified the predicted exponents k according to eq 4,^{46,47} whereas other studies revealed stronger as well as weaker dependencies.^{20,21,26,30,36}

In eq 4, we have explicitly included the P^0 factor to stress that in the case of pure reptation the matrix molecular weight is irrelevant. When other mechanisms of motion, such as constraint release, are taken into account, this prediction is of course no longer valid.

The constraint release mechanism can be avoided completely when the matrix is cross-linked. With regard to the durability of the tube, this corresponds approximately to a matrix with infinite molecular weight, with the additional feature that the junction points are localized chemical bonds instead of vaguely defined entanglements. A cross-linked matrix therefore comes close to de Gennes's original model of an array of fixed obstacles, and studying the diffusion of linear chains in a chemically cross-linked system presents a conceptually simpler way of testing some of the reptation predictions. Direct comparison with a corresponding semidilute solution, on the other hand, can provide valuable additional information.

In the present investigation, we realize the scheme of an unattached chain in a network by enclosing fluorescently labeled polystyrene (PS) tracer molecules in a semidilute, entangled solution of PS matrix polymers. The latter carry photo-cross-linkable groups such that the matrix can be successively cross-linked by UV-irradiation. It is described elsewhere that the cross-linking reaction employed proceeds with high efficiency and that the networks obtained are fairly homogeneous.⁵⁰ FRAP (fluorescence recovery after photobleaching) measurements provide the diffusion coefficient of the labeled tracer chains at every stage of the cross-linking process during the transition from sol to gel. The typical length scale of these FRAP measurements is of the order of 10 μm . This is a macroscopic scale compared to the size of the diffusing species and the structural and topological features of the surrounding medium, particularly network inhomogeneities, whose typical correlation lengths cover a range of 10–100 nm. Hence, we avoid the time and length scales where anomalous diffusion is observed. By using PS as tracer and matrix polymers as well in the good solvent toluene, we expect to minimize specific interactions between tracer and matrix polymers.

This work carries forward several of our recent studies on the dynamics of polymers in semidilute solutions and gels. Liu et al. investigated the tracer diffusion of PS in solutions of PS in toluene by FCS (fluorescence correlation spectroscopy).⁴⁶ The results largely confirm the reptation idea, but fairly high degrees of labeling with rhodamine B had been used. In the present investigation labeling is achieved with 6-(7-nitrobenzofurazan-4-ylamino)hexanoic acid, and degrees of functionalization are kept well below 0.5 mol %. Seiffert et al. studied the tracer dynamics of polyacrylamide in polyacrylamide hydrogels in semidilute solutions and in gels by means of FRAP.⁴² A point of concern in these studies is the polydispersity of the tracers which were obtained via free-radical polymerization. Thus, the inspection of molecular weight dependences was hampered. The currently used PS system is advantageous in that nearly monodisperse samples are readily available over a wide range of molecular weights.

Materials and Methods

Polystyrene Tracer. Linear polymer tracers with molecular weights between $M_w = 123\,000$ and $2\,000\,000$ g/mol were synthesized by a polymer analogous hydroxyalkylation of PS with

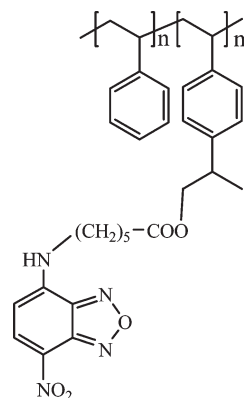


Figure 1. Molecular structure of the tracer copolymer with attached fluorescent dye.

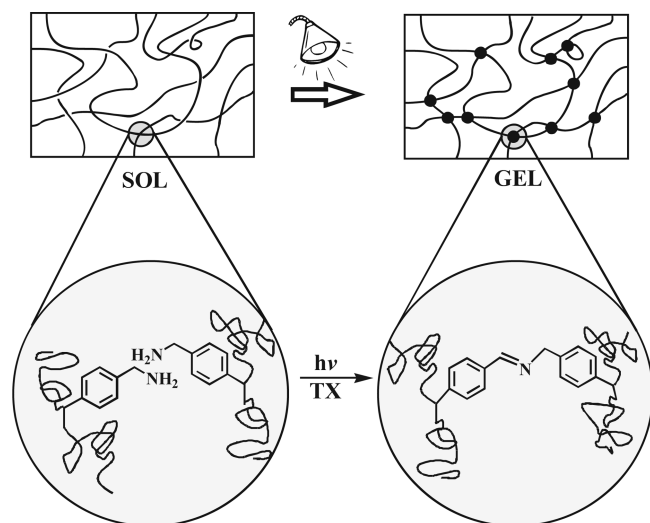
low polydispersity (Pressure Chemicals, Pittsburgh, PA) and subsequent labeling with the fluorescent dye 6-(7-nitrobenzofurazan)hexanoic acid (NBHA).^{51,52}

Poly(styrene-co-(p-(2-hydroxy-isopropyl)styrene)). The hydroxyalkylation of PS was performed by an electrophilic aromatic substitution of PS with propylene oxide: 0.3 g of PS was dissolved in 5 mL of freshly distilled dichloromethane, and 0.17 mL (0.5 mol equiv) of SnCl_4 was added. Then, 2 μL (0.01 mol equiv) of propylene oxide was added, and the reaction mixture was stirred at room temperature for 5–6 h. The solution was diluted with 5 mL of dichloromethane, and the copolymer was precipitated in 100 mL of methanol, filtered, and dried. The conversion of this reaction was about 10–30% having 0.1–0.3% of the phenyl groups hydroxylated. The degree of functionalization was determined by NMR analysis. ^1H NMR (400 MHz, CDCl_3): $\delta = 0.54\text{--}2.30$ (m, CH and CH_2 PS-backbone, CH_3 alkyl), $2.54\text{--}2.92$ (m, CH alkyl), $3.30\text{--}3.68$ (m, CH_2 alkyl), $6.10\text{--}7.39$ ppm (m, $\text{H}_{\text{aromat,PS}}$).

Labeling. The introduced hydroxy groups of the copolymer were used to attach the fluorescent dye to the polymer by Steglich esterification: 0.3 g of hydroxylated copolymer was dissolved in 5 mL of freshly distilled dichloromethane. Then, 10 mol equiv of NBHA with respect to the number of hydroxyl groups, 20 mol equiv of (dimethylamino)pyridine (DMAP), and 10 mol equiv of dicyclohexylcarbodiimide (DCC) were added successively, and the reaction mixture was stirred overnight. Finally, the solution was diluted with dichloromethane to 10 mL, and the yellow polymer was precipitated in 100 mL of methanol. To remove unreacted fluorescent dye, the dissolution and precipitation process was repeated twice. The degree of labeling was determined by UV/vis spectroscopy in tetrahydrofuran (THF) at a maximum absorption of 458 nm (extinction coefficient: $\epsilon = 19\,200$ L/(mol cm)). The degree of functionalization was estimated to 0.1–0.3 mol %. SEC (size exclusion chromatography) analysis of labeled copolymer and pure PS showed no difference in the molar mass distributions indicating unchanged PS properties.

Polystyrene Matrix. Linear PS (Pressure Chemicals, Pittsburgh, PA) with low polydispersities and molecular weights between $M_w = 123\,000$ and $900\,000$ g/mol and a polydisperse PS (BASF, Ludwigshafen, Germany) with $M_n = 160\,000$ g/mol and $M_w/M_n = 2.2$ were converted to cross-linkable P(S-co-AMS) by a two-step polymer analogous reaction.^{53,54}

Poly(styrene-co-(N-methylphthalimide)styrene). In the first step, PS was functionalized with N-methylphthalimide groups by an electrophilic aromatic substitution: 2.5 g of PS was dissolved in 75 mL of freshly distilled dichloromethane, and the solution was put under a nitrogen atmosphere. 44.6 mg (0.01 mol equiv) of N-chloromethylphthalimide and 1.5 mL of SnCl_4 were added, and the reaction mixture was stirred for 5 h at 30°C . A few amounts of THF stopped the reaction, and 125 mL of dichloromethane was added. The copolymer was precipitated in

Scheme 1. Principle of the Photo-Cross-Linking Reaction of P(S-co-AMS)

2 L of methanol, filtered, and dried. The conversion was about 40%, and the degree of functionalization was determined by NMR spectroscopy. ^1H NMR (400 MHz, CDCl_3): δ = 1.02–2.34 (m, CH, and CH_2 PS-backbone), 4.63–4.79 (s, CHN), 6.00–7.39 (m, $\text{H}_{\text{aromat,PS}}$), 7.57–7.90 ppm ($\text{H}_{\text{aromat,phthalimide}}$).

Poly(styrene-co-aminomethylstyrene). 2.5 g of P(styrene-co-(*N*-methylphthalimide)styrene). 2.5 g of P(styrene-co-(*N*-methylphthalimide)styrene) was dissolved in 75 mL of dioxane, and the solution was heated to 30 °C. 5 mL of aqueous methylamine solution (w = 40%) was added dropwise. The reaction mixture was stirred for 72 h at 30 °C. P(S-co-AMS) was precipitated in 800 mL of methanol, filtered, and dried. Full conversion to the aminomethylated product was confirmed by NMR analysis. ^1H NMR (400 MHz, CDCl_3): δ = 1.06–2.31 (m, CH, and CH_2 PS-backbone), 3.65–3.82 (s, CHN), 6.19–7.33 ppm (m, $\text{H}_{\text{aromat,PS}}$). The degree of functionalization was determined to be between 0.37 and 0.56 mol %. Again, no change of the molar mass distribution of copolymer and pure PS was observed by SEC analysis, confirming that the PS properties were not affected by the low degree of functionalization.

Photo-Cross-Linking. Cross-linking of P(S-co-AMS) in semidilute solution in toluene was performed by irradiation with UV light (λ = 370 \pm 18 nm, 100 W Xe arc lamp equipped with band-pass filter) in the presence of thioxanthone as the photoinitiator. The concentration of the copolymers ranged between 75 and 200 g/L, and the concentration of thioxanthone was adjusted so that only 10% of the incident light was absorbed by the sample to avoid formation of a gradient of the irradiation intensity. Scheme 1 shows the principle of the stepwise photo-cross-linking reaction. The gelation process was followed by oscillatory shear experiments on a rheometer (Gemini, Malvern/Bohlin Instruments GmbH) equipped with a quartz glass plate which allows for irradiation of the sample from the bottom during the rheological measurements, and static light scattering (SLS) measurements were performed on a Fica SLS instrument (λ = 632.8 nm) to gain information about the microstructural properties of the gels. The whole cross-linking process and the characterization of the corresponding gels are described elsewhere.⁵⁰

FRAP Measurements. FRAP measurements to determine diffusion coefficients with high spatial and temporal resolution were performed on a Leica TCS SP2 confocal laser scanning microscope (Heidelberg, Germany). All samples were placed in quartz glass cuvettes with a thickness of 100 μm . The confocal plane was adjusted in the middle of the specimen. In the scan mode, the fluorophores were excited with the 458 nm line of an Ar laser at 40–50% of its maximum intensity. For bleaching a point in the confocal plane, a chosen spot was irradiated using the stronger laser lines at wavelengths 476, 488, and 514 nm with

maximum intensity for 0.5–1 s depending on the mobility of the tracer. Subsequent scanning for 15 s to several minutes at suitable time intervals produced around 30 intensity profiles around the bleached spot that represented the diffusion of intact tracer molecules into the bleached area.

A 10 \times DRY objective with a numerical aperture NA = 0.3 was used to ensure that bleaching does not create any distinct gradient in the z -direction, and hence, only two-dimensional diffusion processes have to be considered. Further settings were beam expander = 3 and resolution = 256 \times 256 pixels. Zoom (ranging from 8 to 20, resulting in image sizes from 188 \times 188 μm to 77 \times 77 μm) and line scanning speed (between 400 and 800 Hz) were adjusted for each experiment to get best experimental conditions. It could be shown that varying the parameters in a certain range had no influence on the evaluation procedure. All experiments were performed at 25 °C.

A detailed discussion of the evaluation procedure has been published.⁵⁶ In the following, we just stress the essential points and give an example. The measured intensity profiles were used to determine diffusion coefficients by applying solutions to Fick's second law of diffusion. For a FRAP experiment in the case of two-dimensional diffusion, the equation reads⁵⁵

$$C(r, t) \sim I(r, t) = I_0 - \frac{M}{4\pi D(t + t_0)} e^{-r^2/[4D(t + t_0)]} \quad (5)$$

$C(r, t)$ is the concentration of the fluorophore that is proportional to the (relative) fluorescence intensity $I(r, t)$. M is formally a fluorescence intensity per length corresponding to the amount of fluorophores destroyed by bleaching, $I_0(r, t)$ represents the background intensity at $r \rightarrow \infty$, r is the radial distance from the center of the bleached spot, D is the diffusion coefficient, and t_0 denotes the time lag that has to be introduced because bleaching takes a finite time and so the starting conditions are not exactly defined. Intensity profiles observed at time t are therefore negative Gaussians having a variance $w^2 = 2D(t + t_0)$ and a prefactor proportional to $1/(t + t_0)$. The data points of a complete set of intensity profiles can then be fit to eq 5 to evaluate D . Panels a–d of Figure 2 show, as an example, intensity profiles measured at selected intervals for a PS tracer with M = 390 000 g/mol in a 100 g/L solution of matrix-PS having a molecular weight P = 2 000 000 g/mol. In panel e of Figure 2, w^2 is shown as a function of t . The linearity of the plot proves that the mean-square displacement is linear in time, indicative of normal Fickian diffusion. This applies to all measurements considered in this study.

Equation 5 is only valid in the case of a single diffusing species. A similar fitting procedure assuming a distribution of diffusion coefficients was also applied in order to check for inconsistencies.^{56,57}

Results and Discussion

Polymer Tracer Diffusion in Semidilute Solutions. In the first section we consider briefly the diffusion of tracer polymers in semidilute solution. Although such studies have been made previously (using different polymers and applying different methods) and the general behavior is basically known, we show and discuss our results to provide a sound basis for focusing on the influence of cross-linking of the semidilute matrix in subsequent sections.

We use FRAP to study the diffusion of tracer polystyrenes that are present in a semidilute solution of unmodified polystyrene. The tracer polymers as well as the matrix polymers have a narrow molecular weight distribution, and the molecular weights of both polymers, denoted M for tracer polymers and P for matrix polymers, are varied systematically and independently.

The concentration of the matrix polymers is fixed to c = 100 g/L. This is well above the overlap concentration c^* for

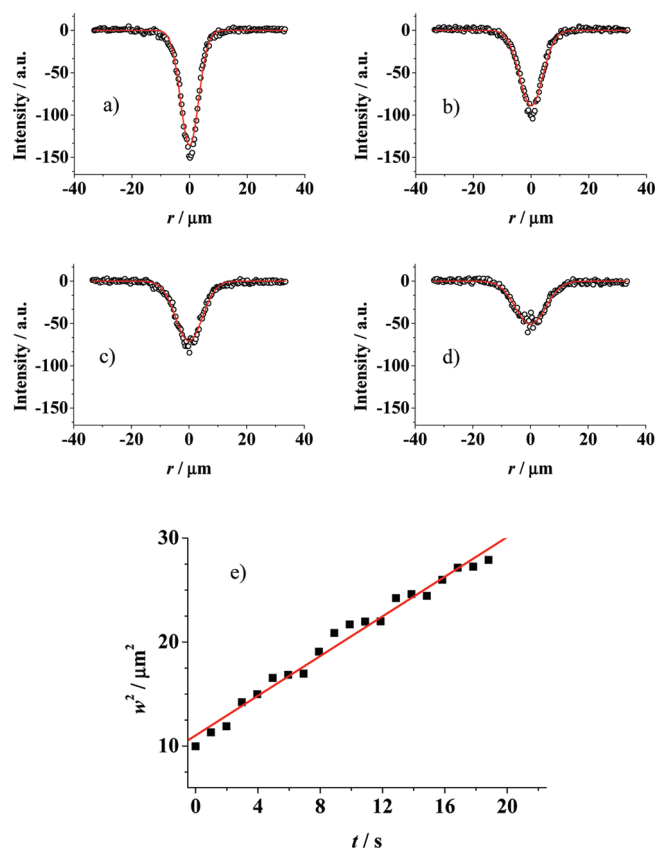


Figure 2. Fluorescence recovery profiles (a) 0, (b) 4.9, (c) 9.9, and (d) 18.8 s after bleaching and variance of Gaussians, w^2 , vs time, t . (e) Measurements shown are for a PS tracer with $M = 390\,000$ g/mol in a 100 g/L solution of matrix-PS having molecular weight $P = 2\,000\,000$ g/mol.

Table 1. Overlap Concentrations, $c^* = 3P/(4\pi N_A R_g^3)$, $R_g^2 = 1.38 \times 10^{-4} P^{1.19} \text{ nm}^2$ According to Ref 59

matrix molecular weight P , g/mol	overlap conc c^* , g/L
50 000	50
123 000	25
200 000	17
390 000	10
900 000	5.2
2 000 000	2.8

all polymers studied; hence, we call the solution semidilute. However, the ratio c/c^* rises upon increasing the molecular weight of the matrix polymers because c^* decreases with increasing molecular weight. In case of the shortest matrix chains, $P = 50\,000$ g/mol, the ratio c/c^* reaches just 2, while c/c^* is about 50 when $P = 2\,000\,000$ g/mol. Overlap concentrations c^* for all matrix polymers employed are listed in Table 1. Note that chain entanglement only occurs at concentrations c_e significant larger than c^* . In good solvents, $c_e \approx 5c^* - 10c^*$ seems to be a good estimate.⁵⁻⁷

The concentration of the tracer polymers was adjusted to 0.5–1 g/L, which is well below their overlap concentration. The system studied thus consists of a dilute solution of tracer polymers in a semidilute matrix. Of course, there is overlap of the tracer polymers with matrix polymers.

The dependence of the tracer diffusion coefficients D on the molecular weights of tracer polymers and matrix polymers are shown in Figures 3 and 4, where Figure 3 depicts the P dependence for various tracer polymers and Figure 4 depicts the M dependence for a series of matrices. Recall

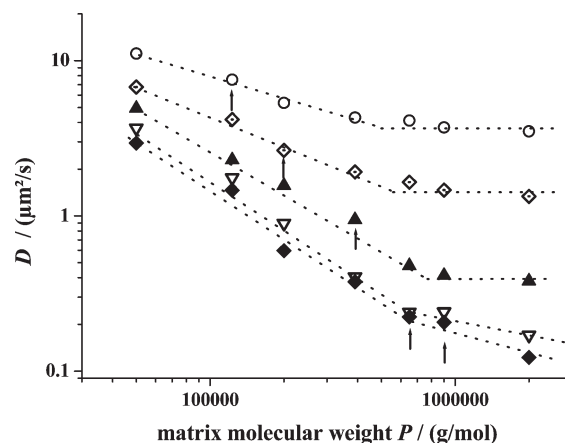


Figure 3. Dependence of the diffusion coefficient of several polymer tracers on matrix molecular weight P in semidilute solution, $c = 100$ g/L. Tracer molecular weights M : (○) 123 000, (□) 200 000, (▲) 390 000, (▽) 650 000, and (◆) 900 000 g/mol. Arrows indicate the situation $M = P$.

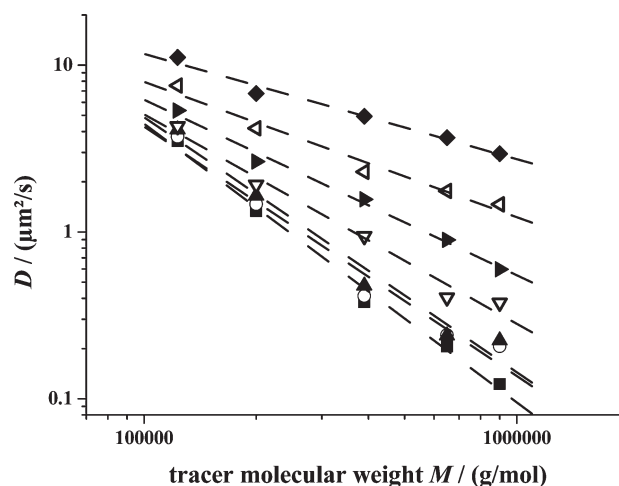


Figure 4. Dependence of the tracer diffusion coefficient on the molecular weight of the tracer polymers for different molecular weights of the matrix polymers at $c = 100$ g/L. Molecular weight P of matrix polymers: (◆) 50 000, (tilted △) 123 000, (tilted ▲) 200 000, (▽) 390 000, (▲) 650 000, (○) 900 000, and (■) 2 000 000 g/mol.

that pure reptation predicts a $P^0 M^{-2}$ dependence. Obviously, strong deviations from this prediction are observed; hence, the tracer dynamics in the systems studied does not occur solely by reptation.

In Figure 3 we recognize two regimes: at low matrix molecular weights, D decreases with rising P , while at the highest matrix molecular weights, D appears to be nearly independent of P within the limits of experimental error. The arrows highlight the self-diffusion case where $P = M$, as opposed to tracer diffusion represented by the other data points.

D being roughly independent of P is only observed when $P \gg M$. This is in accord with literature, where $P \approx 5M$ was specified as the lower limit for the molecular weight of the matrix chains in order to build up topological constraints that are long-living compared to the reptation time of the tracer molecules.¹² Below this threshold, the diffusion coefficient rises with decreasing molecular weight of the matrix polymer, presumably because the constraint-release mechanism becomes dominant. Note that the slope in the double-logarithmic D vs P plots changes from approximately -0.5 to -1 as the molecular weight of the tracer polymers increases from 123 000 to 650 000 g/mol or higher.

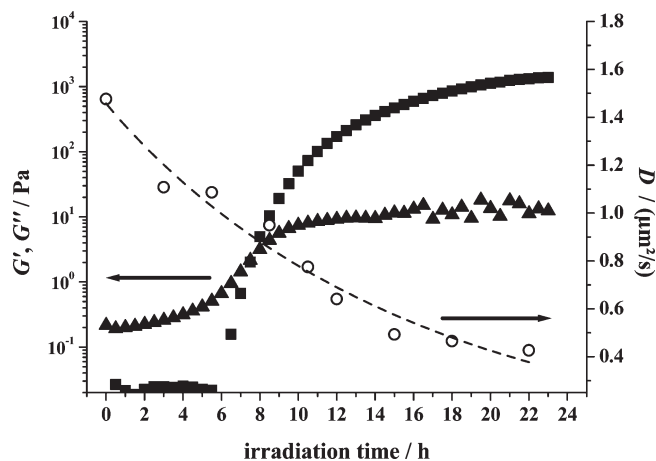


Figure 5. Dependence of the rheological parameters G' (■) and G'' (▲) measured at 1 Hz and of the diffusion coefficient D (○) on irradiation time. PS tracer: $M = 390\,000$ g/mol; P(S-co-AMS) matrix: $P = 200\,000$ g/mol; matrix concentration: $c = 100$ g/L.

Figure 4 is an alternative presentation of the same data set where the focus is on the M dependence of the diffusion coefficient. In a fairly large body of literature a scaling relationship close to $D \sim M^{-2}$ was found, even in fairly dilute solutions where the significance of reptation can be questioned. Our data are characterized by a gradual decrease of the scaling exponent as the matrix molecular weight increases from $P = 50\,000$ g/mol (exp: -0.6) to $P = 2\,000\,000$ g/mol (exp: -1.7). Thus, within the parameter space covered, substantial deviations from the reptation prediction are observed. However, the reptation prediction is approached when the matrix chains are very long, in particular when, additionally, $P \gg M$. Note that the experimental uncertainty of the scaling exponent is approximately ± 0.3 .

Variation of the Diffusion Coefficient of Tracer Polymers When the Matrix Passes through a Sol–Gel Transition. Experiments similar to the ones just described were conducted where the matrix polymers were replaced by P(S-co-AMS), so that the matrix polymers could be cross-linked by UV-irradiation at 370 nm. The irradiation was interrupted at certain intervals, and the diffusion coefficient of the tracer polymers was measured at these particular stages of cross-linking employing the FRAP technique. In a parallel experiment, rheological measurements were performed during the irradiation of the sample to obtain a macroscopic measure of the progress of the cross-linking reaction.

In a typical example, Figure 5 shows the results obtained with matrix chains having $P = 200\,000$ g/mol and tracer chains having $M = 390\,000$ g/mol. For the first 6 h of irradiation, the storage modulus G' remains immeasurably small while the loss modulus G'' shows a moderate rise. Subsequently, G' shoots up several orders of magnitude and finally reaches a plateau value of the order of several kPa after some 20 h of irradiation. G'' also levels off on a value of about 1% of G' . At ~ 8 h, the G' and G'' curves intersect. This point can be taken as a good estimate of the gelation threshold or gel point. While the macroscopic elastic properties show a distinct discontinuity, the diffusion coefficient of the tracer polymers decreases gradually with irradiation time. Cross-linking of the matrix thus has a significant influence on the diffusion coefficient, but the gel point is not at all noticeable in the course of D vs irradiation time.

At the beginning of the cross-linking reaction, the originally linear and monodisperse matrix chains are progressively linked together to form a highly polydisperse mixture of

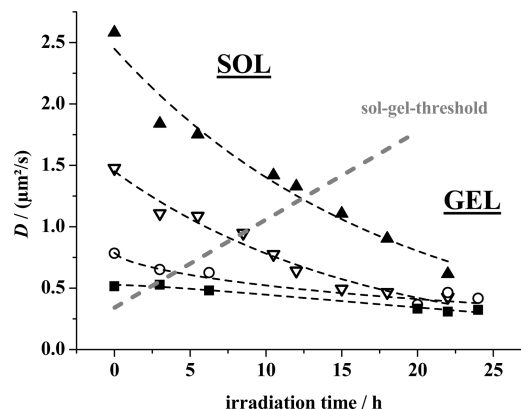


Figure 6. Comparison of the diffusion coefficients of a polymer tracer with $M = 390\,000$ g/mol $^{-1}$ in matrices having different molecular weights, as a function of progressive cross-linking; $c = 100$ g/L $^{-1}$. Matrix molecular weight P : (▲) 123 000, (▽) 200 000, (○) 390 000, and (■) 900 000 g/mol $^{-1}$. Line indicates $G' = G''$ (\approx gelation threshold).

branched macromolecules. The increase of molecular weight as well as the branching results in a reduction of the mobility of the matrix as seen in the rise of G'' (equivalent to viscosity), which enhances the effect of topological constraints imposed on the tracer polymers. Therefore, the tracer diffusion coefficient decreases. At the gel point, one branched structure has grown to span the whole sample. However, this fact is not of any importance for the local environment of each tracer chain. Rather the still increasing molecular weight of the surrounding matrix molecules continuously raises the lifetime of the topological constraints so that the situation pictured by pure reptation, namely an array of fixed obstacles, is finally approached, and the diffusion coefficient assumes a limiting value solely determined by the molecular weight of the tracer molecules.

To confirm this view, Figure 6 shows the dependence of the diffusion coefficient of the tracer polymer with $M = 390\,000$ g/mol on irradiation time, when embedded in matrices having different initial molecular weights P ranging from 123 000 to 900 000 g/mol at a constant matrix concentration of $c = 100$ g/L. In each case, D decreases during the cross-linking process. The decay is strong when the initial molecular weight of the polymer matrix is small, and it is barely perceptible when the polymer matrix has a high initial molecular weight. The final values approached after sufficient irradiation time seem to be virtually identical. This proves that after complete cross-linking practically identical networks are formed irrespective of the initial molecular weight of the matrix chains. (There must be minor variations due to slightly different degrees of amino functionalization and different numbers of chain ends, but this is negligible compared to the experimental uncertainty in D .) When the initial matrix molecular weight is $P = 900\,000$ g/mol, $P > M$ and hence the matrix forms long living entanglements acting as topological constraints on the tracer chains. The situation barely changes upon cross-linking of the matrix, and thus only a minor decrease of D is observed. In contrast, when $P = 123\,000$ g/mol, $P < M$ and the un-cross-linked matrix chains are highly mobile as compared to the tracer chains. Thus, the constraint release mechanism dominates the dynamics, and a much larger tracer diffusion coefficient is observed. Successive cross-linking of this matrix reduces its mobility markedly and therefore has a pronounced effect on D , as seen in Figure 6.

The change of the diffusion coefficient during the photo-cross-linking process thus depends on the ratio of the

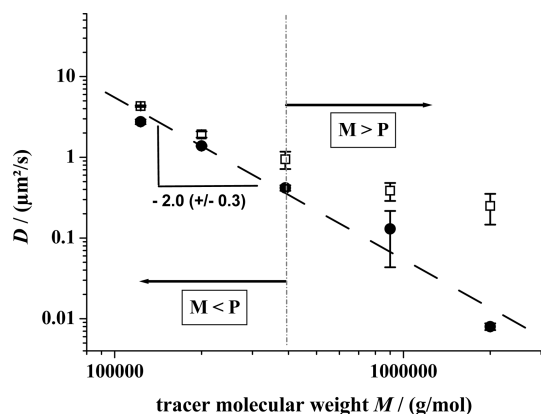


Figure 7. Dependence of the diffusion coefficient on the molecular weight of the polymer tracers in P(S-co-AMS) with $P = 390\,000\text{ g mol}^{-1}$; $c = 100\text{ g L}^{-1}$; □: sol state (before photo-cross-linking); ●: gel state (after photo-cross-linking).

molecular weights of tracer and matrix polymers in the initial sol. If the matrix polymers are already appreciably longer than the tracer polymers, the lifetime of topological constraints is long compared to the reptation time of the tracer molecules. Network formation renders the former even longer, but this cannot affect the tracer diffusion significantly since it is controlled by the latter. In the opposite case, $P < M$, the lifetime of topological constraints exerted by the matrix polymers is short initially but steadily growing with progressive cross-linking. Thus, the tracer diffusion coefficient decreases until the lifetime of the constraints is long enough so that the reptation time of the tracer polymers becomes the dominant factor controlling their diffusion.

So far, we considered the dependence of the diffusion coefficient of one particular tracer polymer on the initial chain length of the matrix polymers and on the effect of cross-linking them. We now focus on a variation of the tracer molecular weight and select one matrix polymer, namely the one having $P = 390\,000\text{ g/mol}$, for that purpose. The matrix concentration is again $c = 100\text{ g/L}$, which means we have $c/c^* \approx 10$ in the un-cross-linked state. Diffusion coefficients were measured by FRAP at different stages of the network formation process. For better clarity, only the diffusion coefficients in the initial, un-cross-linked state and in the completely cross-linked state (after 24 h of irradiation) are depicted in Figure 7.

Expectedly, the reduction of the diffusion coefficient due to cross-linking of the matrix polymer is largest for the longest tracer molecules ($M = 2\,000\,000\text{ g/mol}$). In this case, the lifetime of topological constraints is much shorter than the reptation time of the tracers as long as the matrix remains un-cross-linked. The situation is inverted after complete cross-linking. With somewhat shorter tracer molecules, the initial discrepancy between the two characteristic time scales is not so large; hence, the change of D upon cross-linking becomes smaller. When $M < P$, the reptation time is the essential quantity determining D before and after cross-linking of the matrix, and the effect of cross-linking is rather small.

In view of these remarks, it is readily understood that the gap between the tracer diffusion coefficients measured in the un-cross-linked and cross-linked states widens when the molecular weight of the tracer polymers increases, in particular when $M > P$. As an important feature of Figure 7 we note that the slope of the best fit straight line (shown as a dashed line) describing the course of D vs M in the completely cross-linked matrices is 2.0 ± 0.3 , which confirms exactly

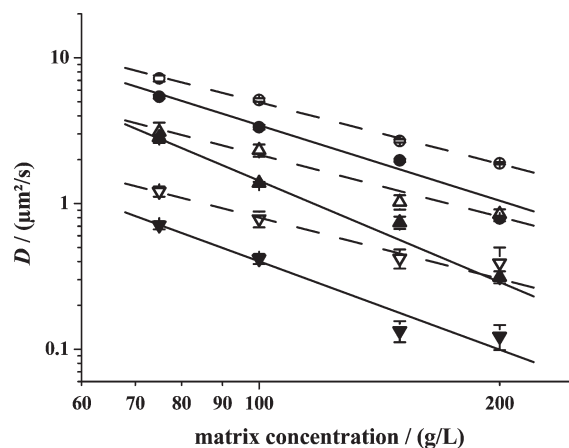


Figure 8. Dependence of the diffusion coefficient of several tracer polymers on the concentration of the P(S-co-AMS) matrix with $P = 390\,000\text{ g/mol}$ in the sol state (open symbols) and in the gel state (filled symbols). Molecular weight of the tracer polymers: (○, ●) 123 000, (△, ▲) 200 000, and (▽, ▼) 390 000 g mol^{-1} .

the reptation prediction. This means that the reptation model can successfully describe the tracer dynamics in the semidilute state, provided that the tracer chains are sufficiently long and the matrix consist of a permanent network or a temporary network whose junctions have a lifetime appreciably longer than the reptation time of the tracers.

In the literature a lot of studies can be found that deal with this topic, and the different working groups determined several dependencies of the diffusion coefficient on the molecular weight of the tracer polymers.^{12,18,20,21,25,26,32,35,36} Exponents with values larger and smaller than -2 were found. Muthukumar tried to explain the differences of these results by performing simulations on the dependence of the tracer dynamics on the structure of the networks.⁵⁸ He carried out computer simulations on probe dynamics in homogeneous and heterogeneous network structures and found out that a stronger dependence of the diffusion coefficient on the molecular weight of the polymer tracer ($D \sim M^{-3}$) is due to a more inhomogeneous structure of the gel. In a fairly homogeneous network, the reptation prediction $D \sim M^{-2}$ is expected.

Dependence of Tracer Dynamics on Matrix Concentration in the Sol and Gel State. Up to now, we only discussed measurements performed in a matrix having a concentration of 100 g/L . We will now focus on the variation of matrix concentration. Three different tracer polymers with $M = 123\,000$, $200\,000$, and $390\,000\text{ g/mol}$ were enclosed in a P(S-co-AMS) matrix with molecular weight $P = 390\,000\text{ g/mol}$. The concentrations of the matrix were chosen as $c = 75$, 100 , 150 , and 200 g/L . We will consider the results of FRAP measurements performed in the un-cross-linked (sol) and in the completely cross-linked (gel) state. Recall that the overlap concentration of this matrix polymer is $c^* = 10\text{ g/L}$; thus, all solutions studied are in the semidilute, entangled regime. When the matrix is fully cross-linked, the network densities of the resulting gels vary roughly in proportion with matrix concentration. (This was proven by modulus measurements.)

In Figure 8, the data sets presented by open symbols and dashed lines show the dependence of the diffusion coefficients of the tracer polymers on matrix concentration in the sol state. The data are well described by a scaling relation $D \sim c^{-k}$ with $k = 1.40 \pm 0.15$. The scaling exponent is identical for the three tracer polymers studied. It is, however, distinctly smaller than the value claimed by reptation theory (1.75 in good solvents).

This behavior may be due to the fact that the crucial ratio of the molecular weights of matrix and tracer polymers is $P/M < 5$ in each case, meaning that the lifetime of the topological constraints is too short to account for pure reptative motion. This view is supported by considering the dependence of D on tracer molecular weight. Vertical sections at each concentration in Figure 8 give slopes between -1.35 and -1.62 for double-logarithmic D vs M plots (instead of -2 predicted for pure reptation) in accord with our earlier discussion (cf. Figure 4).

Upon cross-linking of the matrix polymers, all tracer diffusion coefficients are reduced. This is shown by the filled data points and full lines in Figure 8. The reduction (compared to the sol state) is greater, the longer the tracer chains and the higher the matrix concentration. The former relation has been discussed above and is likely due to the fact that the P/M ratio decreases and approaches unity when tracer polymers in the succession 123 000, 200 000, and 390 000 g/mol are considered. The concentration dependence is far more difficult to comprehend. For tracer diffusion in cross-linked matrices, the scaling exponent k varies unsystematically between 1.7 and 2.3 with an uncertainty of ± 0.3 due to a much higher scatter of the data points. This seems to be close to the reptation prediction, but somewhat too high. It is tempting to interpret this exponent by referring to the marginal solvent regime. However, since the concentration range is limited and we encounter substantial experimental scatter, we have to refrain from an in-depth interpretation. At the same time, the dependence of the diffusion coefficient on the molecular weight of the tracer chains is at all concentrations stronger in the gel than in semidilute solution. Dependencies between $D \sim M^{-1.6}$ and $D \sim M^{-2.3}$ are determined, which again come closer to the predicted $D \sim M^{-2}$ relation.

Conclusions

This study focuses on the effect of cross-linking of a semidilute polymer solution on the dynamics of enclosed linear macromolecules. Linear polystyrene chains having a narrow molecular weight distribution were labeled with a fluorescent dye. Their diffusion coefficient was determined by FRAP when such chains were embedded in a semidilute matrix of polystyrene in toluene. The matrix polymers used were suitably functionalized such that they could be photo-cross-linked without attachment of the tracer chains.

The results obtained enable us to discuss and compare in detail some peculiarities of tracer dynamics in a solution and in a cross-linked gel under identical conditions. In semidilute solution, significant deviations from the reptation predictions appear: The tracer diffusion coefficient shows a marked dependence on the molecular weight of the matrix chains, unless a threshold value $P \approx 5M$ is exceeded. Second, the molecular weight dependence of the tracer diffusion coefficient is weaker than the $D \sim M^{-2}$ prediction. Third, the dependence of D on matrix concentration is also weaker than predicted. These experimental facts largely agree with what is known from the literature.

Cross-linking of the matrix chains results in a more or less pronounced decrease of the tracer diffusion coefficient. The change occurs gradually with rising conversion of the cross-linking reaction, without any singularity at the macroscopically observed gel point. A significant drop of D upon cross-linking of the matrix is observed when $P < M$ initially, while the decrease is hardly perceptible in a matrix of very long chains. When the matrix chains are finally cross-linked to form a gel of sufficiently high network density, the diffusion coefficient of the linear tracers virtually follows the predictions of reptation theory: We observe

$D \sim M^{-2}$ and $D \sim c^{-(2.0 \pm 0.3)}$, keeping in mind the reservation about the scatter of data as mentioned above. What can be stated beyond doubt, however, is that upon cross-linking of the matrix the dependencies of the tracer diffusion coefficient on tracer molecular weight, on the one hand, and on matrix concentration, on the other hand, converge to what is predicted by reptation theory.

These findings suggest the notion that in a gel reptation is the dominant mechanism of tracer dynamics, while in solution additional processes contribute to chain mobility. The resulting diffusion coefficient in a solution is therefore larger than that of the same tracer in a gel. Its rise is becoming more distinct with lower molecular weight of the matrix chains. This is a strong indication of the fact that the constraint release mechanism plays an essential role. Successive cross-linking of the matrix gradually raises the lifetime of the topological constraints, thus lowering the tracer diffusion coefficient until it finally approaches the value defined by pure reptation, in full agreement with our experimental results. This picture seems to be valid in the semidilute solution regime at concentrations on the order of 10%.

Acknowledgment. Financial support for this study from the German Science Foundation (DFG) is gratefully acknowledged.

References and Notes

- (1) De Gennes, P. G. *J. Chem. Phys.* **1971**, *55*, 572–579.
- (2) De Gennes, P. G. *Macromolecules* **1976**, *9*, 587–593.
- (3) De Gennes, P. G. *Macromolecules* **1976**, *9*, 594–598.
- (4) De Gennes, P.-G. *Scaling Concepts in Polymer Physics*; Cornell University Press: Ithaca, NY, 1991.
- (5) Lodge, T. P.; Rotstein, N. A.; Prager, S. *Adv. Chem. Phys.* **1990**, *79*, 1–132.
- (6) Graessley, W. W. *Polymeric Liquids & Networks: Dynamics and Rheology*; Garland Science: New York, 2008.
- (7) Rubinstein, M.; Colby, R. *Polymer Physics*; Oxford University Press: New York, 2008.
- (8) Doi, M. *J. Polym. Sci., Part C: Polym. Lett.* **1981**, *19*, 265–273.
- (9) Zamponi, M.; Monkenbusch, M.; Willner, L.; Wischniewski, A.; Farago, B.; Richter, D. *Europhys. Lett.* **2005**, *72*, 1039–1044.
- (10) Mark, J. E. *Physical Properties of Polymers*; Cambridge University Press: Cambridge, 2004.
- (11) Marmonier, M. F.; Leger, L. *Phys. Rev. Lett.* **1985**, *55*, 1078–1081.
- (12) Nemoto, N.; Kojima, T.; Inoue, T.; Kishine, M.; Hirayama, T.; Kurata, M. *Macromolecules* **1989**, *22*, 3793–3798.
- (13) Schaefer, D. W. *J. Polym. Sci., Polym. Symp.* **1985**, 121–131.
- (14) Schaefer, D. W. *Polym. Prepr.* **1982**, *23*, 53.
- (15) Won, J.; Onyenemezu, C.; Miller, W. G.; Lodge, T. P. *Macromolecules* **1994**, *27*, 7389–7396.
- (16) Antonietti, M.; Coutandin, J.; Sillescu, H. *Macromolecules* **1986**, *19*, 793–798.
- (17) Nemoto, N.; Kishine, M.; Inoue, T.; Osaki, K. *Macromolecules* **1990**, *23*, 659–664.
- (18) Nemoto, N.; Kishine, M.; Inoue, T.; Osaki, K. *Macromolecules* **1991**, *24*, 1648–1654.
- (19) Antonietti, M.; Sillescu, H. *Macromolecules* **1985**, *18*, 1162–1166.
- (20) Kim, H. D.; Chang, T. Y.; Yohanan, J. M.; Wang, L.; Yu, H. *Macromolecules* **1986**, *19*, 2737–2744.
- (21) Wesson, J. A.; Noh, I.; Kitano, T.; Yu, H. *Macromolecules* **1984**, *17*, 782–792.
- (22) Pajevic, S.; Bansil, R.; Konak, C. *J. Non-Cryst. Solids* **1991**, *131*, 630–634.
- (23) Pajevic, S.; Bansil, R.; Konak, C. *Macromolecules* **1993**, *26*, 305–312.
- (24) Bansil, R.; Pajevic, S.; Konak, C. *Macromolecules* **1990**, *23*, 3380–3382.
- (25) Martin, J. E. *Macromolecules* **1984**, *17*, 1279–1283.
- (26) Wheeler, L. M.; Lodge, T. P. *Macromolecules* **1989**, *22*, 3399–3408.
- (27) Rotstein, N. A.; Lodge, T. P. *Macromolecules* **1992**, *25*, 1316–1325.
- (28) Kuo, C. S.; Bansil, R.; Konak, C. *Macromolecules* **1995**, *28*, 768–770.
- (29) Zuo, J.; Huang, J. F.; An, Y. L.; Li, F. X.; Zhu, C. Y.; Zhang, J.; Zhang, Z. G.; He, B. L. *J. Appl. Polym. Sci.* **2002**, *86*, 2062–2066.

- (30) Meistermann, L.; Duval, M.; Tinland, B. *Polym. Bull.* **1997**, *39*, 101–108.
- (31) Onyenemezu, C. N.; Gold, D.; Roman, M.; Miller, W. G. *Macromolecules* **1993**, *26*, 3833–3837.
- (32) Wheeler, L. M.; Lodge, T. P.; Hanley, B.; Tirrell, M. *Macromolecules* **1987**, *20*, 1120–1129.
- (33) Won, J.; Lodge, T. P. *J. Polym. Sci., Part B: Polym. Phys.* **1993**, *31*, 1897–1907.
- (34) Lodge, T. P.; Markland, P.; Wheeler, L. M. *Macromolecules* **1989**, *22*, 3409–3418.
- (35) Lodge, T. P.; Rotstein, N. A. *J. Non-Cryst. Solids* **1991**, *131*, 671–675.
- (36) Fleischer, G.; Zgadzai, O. E.; Skirda, V. D.; Maklakov, A. I. *Colloid Polym. Sci.* **1988**, *266*, 201–207.
- (37) Nyden, M.; Soderman, O. *Macromolecules* **1998**, *31*, 4990–5002.
- (38) Nyden, M.; Soderman, O.; Karlstrom, G. *Macromolecules* **1999**, *32*, 127–135.
- (39) Kamiguchi, K.; Kuroki, S.; Satoh, M.; Ando, I. *Polymer* **2005**, *46*, 11470–11475.
- (40) Kamiguchi, K.; Kuroki, S.; Satoh, M.; Ando, I. *Macromolecules* **2008**, *41*, 1318–1322.
- (41) Kamiguchi, K.; Kuroki, S.; Satoh, M.; Ando, I. *Macromolecules* **2009**, *42*, 231–235.
- (42) Seiffert, S.; Oppermann, W. *Polymer* **2008**, *49*, 4115–4126.
- (43) De Smedt, S. C.; Meyvis, T. K. L.; Demeester, J.; Van Oostveldt, P.; Blonk, J. C. G.; Hennink, W. E. *Macromolecules* **1997**, *30*, 4863–4870.
- (44) Cheng, Y.; Prud'homme, R. K.; Thomas, J. L. *Macromolecules* **2002**, *35*, 8111–8121.
- (45) Doucet, G. J.; Dorman, D.; Cueto, R.; Neau, D.; Russo, P. S. *Macromolecules* **2006**, *39*, 9446–9455.
- (46) Liu, R. G.; Gao, X.; Adams, J.; Oppermann, W. *Macromolecules* **2005**, *38*, 8845–8849.
- (47) Cherdhirankorn, T.; Best, A.; Koynov, K.; Peneva, K.; Muellen, K.; Fytas, G. *J. Phys. Chem. B* **2009**, *113*, 3355–3359.
- (48) Zettl, H.; Hafner, W.; Boker, A.; Schmalz, H.; Lanzendorfer, M.; Muller, A. H. E.; Krausch, G. *Macromolecules* **2004**, *37*, 1917–1920.
- (49) Smith, D.; Perkins, T.; Chu, S. *Phys. Rev. Lett.* **1995**, *75*, 4146–4149.
- (50) Susoff, M.; Oppermann, W. *Macromolecules* **2009**, *42*, 9195–9198.
- (51) Park, B. D.; Lee, H. I.; Ryoo, S. J.; Lee, Y. S. *Tetrahedron Lett.* **1997**, *38*, 591–594.
- (52) Neises, B.; Steglich, W. *Angew. Chem., Int. Ed.* **1978**, *17*, 522–524.
- (53) Russ, T.; Brenn, R.; Geoghegan, M. *Macromolecules* **2003**, *36*, 127–141.
- (54) Liu, R. G.; Oppermann, W. *Macromolecules* **2006**, *39*, 4159–4167.
- (55) Crank, J. *The Mathematics of Diffusion*; Oxford University Press: London, 1957.
- (56) Seiffert, S.; Oppermann, W. *J. Microsc. (Oxford, U. K.)* **2005**, *220*, 20–30.
- (57) Hauser, G. I.; Seiffert, S.; Oppermann, W. *J. Microsc. (Oxford, U. K.)* **2008**, *230*, 353–362.
- (58) Muthukumar, M. *J. Non-Cryst. Solids* **1991**, *131*, 654–666.
- (59) Higo, Y.; Ueno, N.; Noda, I. *Polym. J.* **1983**, *15*, 367–375.